

Atmospheric Chemical Composition Response to Energetic Electron Precipitations



Dmitry Grankin , Irina Mironova , and Eugene Rozanov 

Abstract Energetic particle precipitation (EPP) can affect the chemical composition of the Earth's atmosphere. Particles emitted by the Sun in the form of the solar wind (SW) reach the Earth's magnetosphere, accelerate to high energies, and reach the dense layers of the atmosphere, triggering chains of chemical reactions that lead to a change in the chemical composition of the atmosphere, thereby EPP leads to ionization of the atmosphere. In this paper, we considered the response of the atmosphere to energetic electron precipitation (EEP) in a high-latitude atmosphere above Apatity (67.57°N, 33.56°E, L = 5.3). We exploited two versions of a one-dimensional radiative-convective model of the atmosphere with interactive neutral and ionic chemistry. The first version calculates the production of primary radicals as a function of ionization rate and altitude; the second, introduced by us—additionally includes treatment of the complete ion chemistry. The models gave results which were compared in the paper.

Keywords Energetic electron precipitation · Atmospheric chemistry modeling · Ozone depletion

D. Grankin (✉) · I. Mironova · E. Rozanov
Saint Petersburg State University, Universitetskaya emb., 7-9, St. Petersburg 199034, Russia
e-mail: d.grankin@spbu.ru

I. Mironova
e-mail: i.a.mironova@spbu.ru

E. Rozanov
e-mail: eugene.rozanow@pmodwrc.ch

E. Rozanov
Physikalisch-Meteorologisches Observatorium Davos (PMOD/WRC), Dorfstrasse 33, 7260
Davos Dorf, Switzerland

1 Introduction

Energetic particle precipitation (EPP) plays an important role in changing the chemical composition of the Earth's atmosphere [1–3]. Particles emitted by the Sun in the form of the solar wind (SW) reach the Earth's magnetosphere, accelerate to high energies and reach the dense layers of the atmosphere, triggering chains of chemical reactions that lead to a change in the chemical composition of the atmosphere, especially during the polar winter periods, when the effect of solar radiation is minimal and vertical transport of the resulting chemically active species is possible. Thus, considering these periods, the effects associated with EPP can be observed.

It is known that EPP leads to ionization of the atmosphere [3–6]. EPP events can be very different due to many factors: the cause of occurrence (that is, considering the cause of precipitation, for example, a solar proton event, a coronal hole, etc.); the energy spectrum; the energetic particles reference to solar activity; the geographic location of the impact on the atmosphere (i.e., the location of the precipitation).

Energetic particles such as electrons, protons, alpha particles and other heavier elements (quite rare) are ejected from the surface of the Sun. While high-energy protons can reach the polar regions, where the magnetic field is weakened, electrons, in order to precipitate into the atmosphere, need some acceleration, which is obtained in the magnetosphere. In this paper, we study the effect of EEP (energetic electron precipitation) on the Earth's atmosphere, since electron precipitation occurs regularly, and intense proton events are rather rare phenomena [7]. In this regard, it is the precipitation of magnetospheric electrons that has the most significant impact on the chemistry of the atmosphere in the long term.

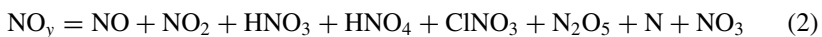
Let us consider the main chemical compounds and reactions occurring after the precipitation of energetic particles. Ionization of neutral molecules by energetic particles leads to the activation of a chain of complex ionic reactions, which eventually produce such important products for atmospheric chemistry as nitrogen and hydrogen oxides [1, 2].

The so-called odd hydrogen group (or family of hydrogen-containing radicals) HO_x includes the following components: hydrogen, hydroxyl, and hydroperoxide [1, 2]:



The lifetime of such radicals is short (minutes) [4]. It is directly proportional to the mass density of the substance, also it is a measure of the time required for the mass density of a compound to decrease by a fraction of e (2.718) if there are no sources. Interacting with mesospheric ozone, HO_x radicals participate in fast chains of chemical reactions at altitudes between 60 and 80 km (D-region of the Earth's ionosphere) [1, 2, 8].

However, there is more long-lived chemical family, such as NO_y :

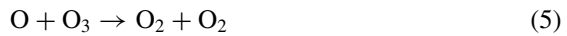


Since NO_y exist longer (hours and months under polar night conditions) [4], these species are subject to movement by air currents, so the effects of the NO_y family exposure can be detected far from the zone of direct ionization and NO_y production.

The depletion of the Earth's ozone layer is known to be affected by precipitation of energetic particles, especially during the polar winter, as described previously. The destruction of ozone in the mesosphere occurs in catalytic cycles. The components of the HO_x and NO_y families are involved in chains of fast reactions leading to the destruction of mesospheric ozone [1–3]:



Net:



Net:



These chemical reactions lead to ozone depletion and can change atmospheric temperature [1, 2]. These are the two most important EPP-related cycles of ozone destruction, the so-called hydrogen and nitrogen catalytic cycles [9].

Ozone absorbs ultraviolet solar radiation and is involved in the long-wave radiation transfer. All changes in the chemical composition of the atmosphere lead to heating and cooling, and ozone losses during periods of strong magnetic storms and solar proton events can reach 40–50% in the upper stratosphere and 80–90% in the mesosphere [1, 2]. The main purpose of this work is to study the precipitation of energetic electrons and their impact on the Earth's polar atmosphere based on two versions of one-dimensional models and compare the results obtained.

Here we study the response of the atmosphere to precipitation of energetic electrons in the high-latitude atmosphere using two versions of the one-dimensional radiative-convective model of the atmosphere with interactive neutral and ion chemistry [11] and obtain information on the response of the atmosphere to precipitation of energetic electrons over Apatity (67.57N, 33.56E, McIlwain parameter $L = 5.3$), where numerous balloon observations were made [10, 12].

2 Model Description

In this work, we used a one-dimensional radiative-convective model with interactive neutral and ionic chemistry [13]. Two versions of the model were used (with parameterized and full ion chemistry). Both models cover a range of heights from 21 to 92 km above the Earth's surface in the study area. We consider changes in the chemical composition of the atmosphere after EEP.

2.1 Parameterized Model

Energetic electrons, protons and the secondary electrons formed by them ionize neutrals which leads to the formation of odd hydrogen HO_x and odd nitrogen NO_y . In the mesosphere, observation of these groups provides an indication of ozone depletion.

NO_y is formed after the collision of the above energetic particles with neutrals and appearance of ionized species.

$$P(\text{N}_2^+) \rightarrow 0.585Q \quad (9)$$

$$P(\text{N}^+) \rightarrow 0.185Q \quad (10)$$

$$P(\text{O}_2^+) \rightarrow 0.154Q \quad (11)$$

$$P(\text{O}^+) \rightarrow 0.076Q, \quad (12)$$

where P is production and Q is ionization rate. Finally, ~ 1.25 N molecules per ion pair [14, 15] are formed:

Further calculations use the following ratios. The ion pair accounts for:

- ~ 0.7 molecules of excited nitrogen $\text{N}(^2\text{D})$, which instantly reacts with neutral oxygen and gives NO:

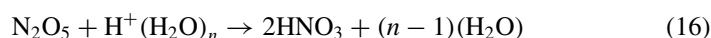
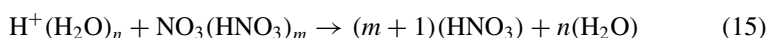
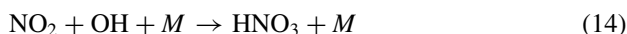


- ~ 0.55 molecules of NO_2

The formation of HO_x is due to complex ionic chemistry. In this version we use the parameterization of HO_x production as a function of the altitude and ionization rate [16]. On average one ion pair produces one H atom and one OH (but this ratio changes with height).

2.2 Ion Chemistry Model

This model version can treat neutral and ion chemistry, including 43 neutral radicals and 57 negatively and positively charged ions [11, 15–17]. In addition to NO_y and HO_x formation in the parameterized version many other neutrals from hydrogen, nitrogen and halogen groups can be formed. For example, nitric acid (HNO_3) can be produced via following reactions:



The number of produced NO_y and HO_x molecules is not fixed, as it was in the parameterized scheme, since additional chemical reactions are now taken into account.

3 Results

To study the effect of EEP on the chemical composition of the atmosphere, we chose one of the EEP events (registered during balloon observations) that occurred on March 7, 2005 (the serial number of the day in the year is 66; $\text{DOY} = 66$, “day of the year” is abbreviated as “DOY”). On this day, a relatively strong geomagnetic disturbance was observed with values of the K_p index of about 6. According to the database [18], the value of the D_{st} index reached -50 nT, the solar wind velocity fluctuated between 600 and 700 km/s, and the B_z component of the interplanetary magnetic field rapidly oscillated between -5.4 and 3.0 nT (Fig. 1).

The ionization rate for investigated period was calculated considering the spectra obtained from the database prepared by the Lebedev Institute of Physics team [10]. The description of the response functions and the basis for calculating the ionization rates are presented in [4–6]. The ionization rate altitude profile is shown at Fig. 2. The graph shows that the production of ion pairs increases with the altitude. The ionization rates represented are in ion pairs per second (ip/s, x-axis).

Let’s consider what happens in the atmosphere the day before the event, during the event we are considering, and after it. The results of the atmospheric response to EEP for NO_y and HO_x are shown in Fig. 3. Further we consider 63 km and 79 km levels because ionization rates at these levels differ one from another greatly.

NO_y is a longer-lived chemical compound comparing to HO_x . The lifetime and amount of molecules of a particular chemical compound is affected by the time during which the event occurs and is considered. Since there is a certain amount of solar

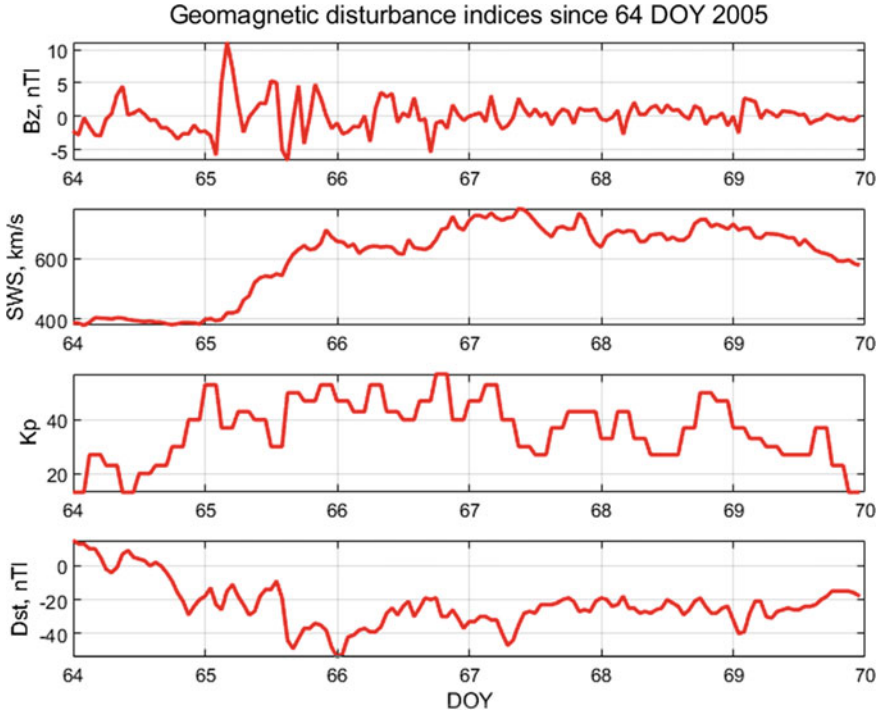


Fig. 1 Bz, SWS and geomagnetic disturbance indices during 5–11 March of 2005. Kp index values are multiplied by 10

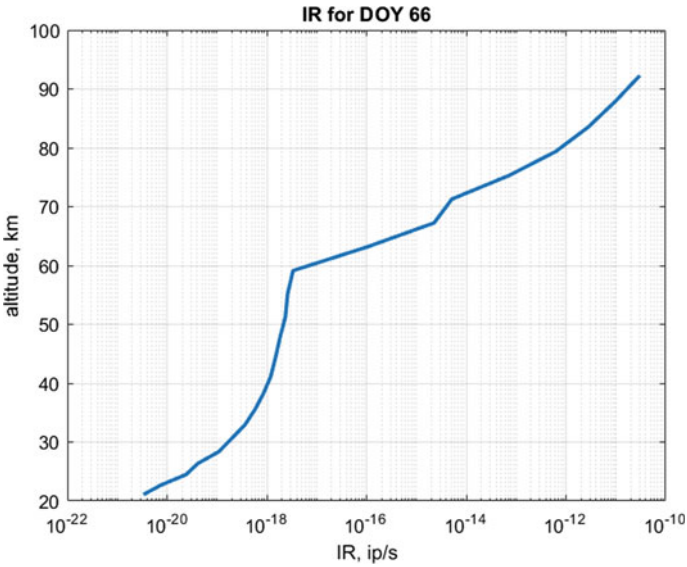


Fig. 2 Altitudinal profile of ionization rate at DOY 66

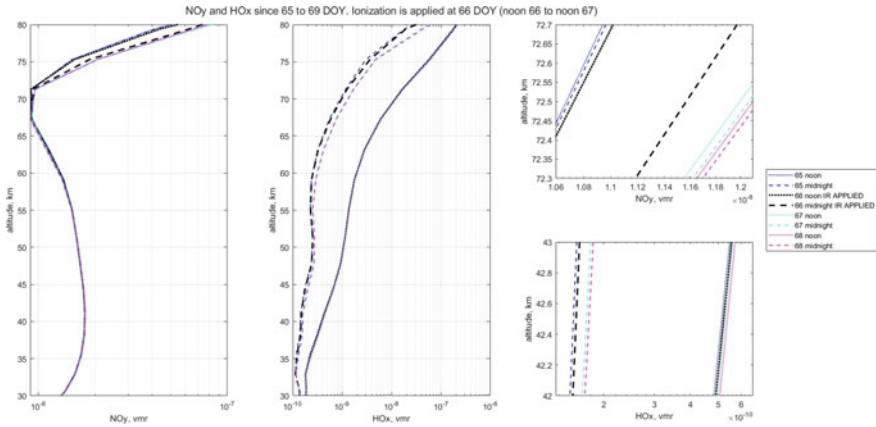


Fig. 3 The content of NO_y and HO_x in the atmosphere at different moments from 65 to 68 days (from March 6 to March 10, 2005). Ionization from the event was applied from noon on day 66 to noon on day 67. The two right panels are indicated to distinguish between the lines shown on the two left panels. The ‘vmr’ unit is the volume mixing ratio

radiation penetrating the atmosphere at noon (March 7—the polar night is coming to an end), the total content of NO_y and HO_x decreases by noon and increases by midnight. On Fig. 3, midday data are indicated by dashed lines with a short stroke, midnight data by dashed lines with a long stroke. The two panels on the left are a complete vertical profile for NO_y and HO_x , and the two panels on the right (one below the other) are presented for a more accurate consideration of the content of certain chemical compounds.

One day before the event, the amount of NO_y (left and right upper panels) is slightly higher during the day than at night. After the event, this gap becomes larger, more noticeable—from 10.6 ppbv during the day to 11.4 ppbv at night. Then, the difference in the content of NO_y during the day and at night gradually decreases after the ionization is turned off—pairs of blue and purple lines clearly indicate this.

As mentioned above, HO_x life time is shorter than NO_y . The total HO_x content increases by several tenths of a ppb by midnight. The presence of ionization leads to an increase in the total content of HO_x in the atmosphere: we see that groups of day and night lines go to increase the content of HO_x . But since the lifetime of HO_x is short, we do not see the same difference between daytime and nighttime data as for NO_y : noon-midnight line pairs do not follow one another.

In addition, this graph reflects information about the content of NO_y and HO_x depending on altitude: with increasing altitude, the volume fraction of HO_x increases, since with increasing altitude, the effect of ionization by energetic particles increases; the NO_y volume fraction reaches minimal values at approximately 70 km level. HO_x has a longer diurnal cycle than NO_y due to its shorter lifetime, and therefore the EEP signal here is much less pronounced in time.

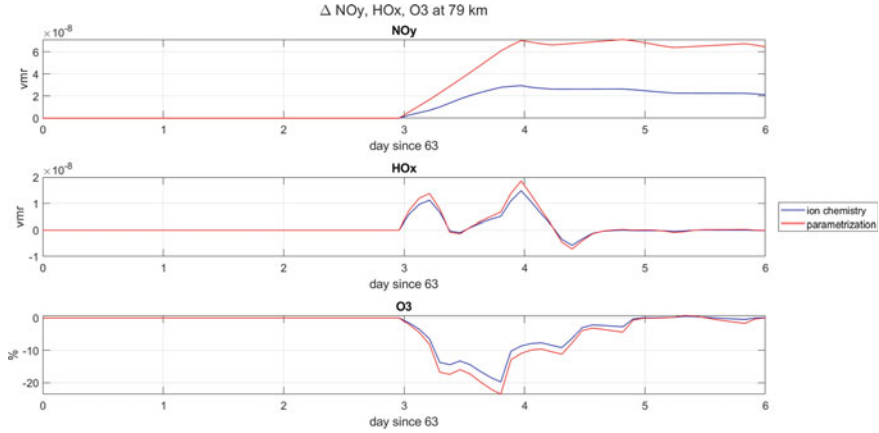


Fig. 4 Effect of precipitation of energetic electrons on NO_y , HO_x and O_3 at the altitude of 79 km. Time from DOY 63, ionization is applied at DOY 66, that is, from day 3 on the charts

According to the catalytic ozone depletion cycles described, ozone depletion is caused by an increase in HO_x and NO_y . The relative change in some physical quantity is calculated according to the formula:

$$\Delta = \frac{\text{experiment} - \text{reference}}{\text{reference}} \cdot 100\% \quad (17)$$

In our case, experiment is the case with introduced ionization (energetic electrons are the source), reference is the case without introducing perturbing ionization. The results obtained by modeling at 79 km are presented as Fig. 4.

Here we clearly see the result of the catalytic cycles. After the event on day 66, there is an increase in HO_x during the daytime, during the night HO_x increases by 20 ppb, which in turn leads to ozone depletion by 20%. The ozone depletion during the daytime begins on the 3rd day. Thus, the precipitation of energetic electrons led to the depletion of the ozone content at 79 km level by 20% compared to the undisturbed conditions in the high-latitude zone. In addition, although the reactions associated with HO_x are fast, as stated; so, we see ozone depletion the next day as the NO_y -related catalytic cycles are already in operation. We see some discrepancy between model versions in the simulation of the NO_y behavior at an altitude of 79 km. The parameterized ion chemistry substantially overestimates NO_y production. However, because of small effects from NO_y at these altitudes the differences in atmospheric ozone response do not exceed 5%. How ozone depletion occurs at other altitudes is shown in Fig. 5 (63 km).

We observe that the total content of HO_x and NO_y changes are lower than at an altitude of 79 km. It happened because of lower ionization rate values for 63 km (see Fig. 2). From this follows a small change in the ozone content: depletion of only a

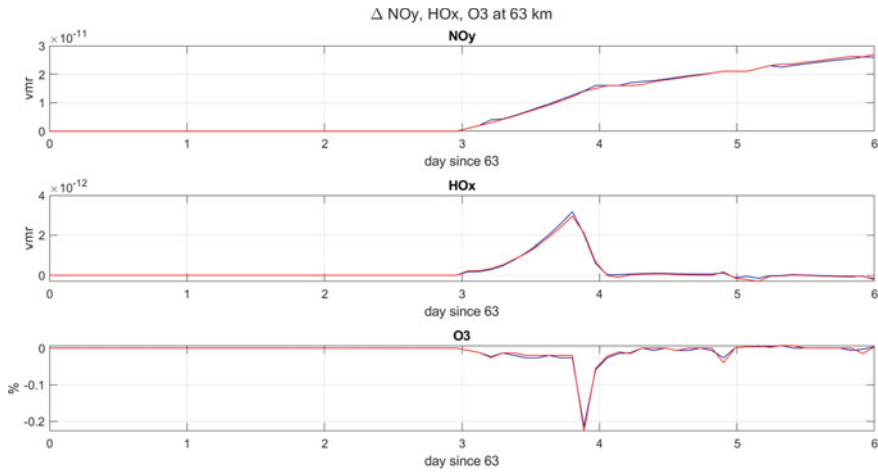


Fig. 5 Influence of precipitation of energetic electrons on NO_y, HO_x and O₃ at a height of 63 km. Time from DOY 63, ionization is applied at DOY 66, that is, from day 3 on the charts

fraction of a percent. However, at these altitudes, both model versions work similarly unlike at upper mesospheric levels.

The ozone response at lower altitudes is not reproduced by 1-D model because the absence of vertical advective transport prevents downward propagation of the enhanced NO_y in the lower thermosphere and mesosphere.

4 Conclusions

In this work, the chemical composition of the atmosphere in the region above Apatity was studied using ionization rates obtained from balloon measurements. To study the impact of energetic electron precipitation on the Earth’s high-latitude atmosphere, we used two versions of a one-dimensional radiative-convective-photochemical model with parameterized and complete ion chemistry. One of the goals was also to compare the results obtained by both versions of the model.

For further analysis, we chose an event that occurred on March 7, 2005 (DOY 66), when the geomagnetic situation was disturbed (see Fig. 1). For this case the model with complete ion chemistry generates the same amount of HO_x but substantially less NO_y in the upper mesosphere, while in the lower mesosphere the results are very similar. The ozone depletion is the same in both cases because it is driven mostly by hydrogen radicals.

Acknowledgements The investigation of the atmospheric chemical composition response to energetic electron precipitations by one-dimensional radiative-convective-photochemical model with parameterized and complete ion chemistry was supported by a grant of the Russian Science Foundation (project no. 20-67-46016). The selection of EEP event detected by balloon observation was

done under the project RFBR № 20-55-12020. The treatment of complete ion chemistry model was done under the project RFBR № 20-05-00450.

This work was carried out at “Ozone layer and upper atmosphere research laboratory” with the support of the Ministry of Science and Higher Education of the Russian Federation under agreement 075-15-2021-583.

References

1. Rozanov, E.V.: Effect of Precipitating Energetic Particles on the Ozone Layer and Climate. *Russ. J. Phys. Chem. B* 12, 786–790 (2018)
2. Matthes K., Dudok T., Lilensten J.: Earth’s climate response to a changing Sun. *EDP Science, Les Ulis*, 267–272 (2015)
3. Mironova I., Karagodin-Doyennel A., Rozanov E.: The Effect of Forbush Decreases on the Polar-Night HO_x Concentration Affecting Stratospheric Ozone. *Front. Earth Sci.* 8, 618583 (2020)
4. Mironova I., Kovaltsov G., Mishev A., Artamonov A.: Ionization in the Earth’s Atmosphere Due to Isotropic Energetic Electron Precipitation: Ion Production and Primary Electron Spectra. *Remote Sensing*, 13 (20), 4161 (2021)
5. Mironova I., Artamonov A., Bazilevskaya G., Rozanov E., Makhmutov V., Mishev A., Karagodin A.: Ionization of the polar atmosphere by energetic electron precipitation retrieved from balloon measurements. *Geophysical Research Letters*, 46, 990–996 (2019)
6. Mironova I., Bazilevskaya G., Kovaltsov G., Artamonov A., Rozanov E., Mishev A., Makhmutov V., Karagodin A., Golubenko K.: Spectra of high energy electron precipitation and atmospheric ionization rates retrieval from balloon measurements. *Science of The Total Environment*, 693, 133242 (2019)
7. Bazilevskaya, G., Logachev, Y., Vashenyuk, E. et al.: Solar proton events in solar activity cycles 21–24. *Bull. Russ. Acad. Sci. Phys.* 79, 573–576 (2015)
8. Brasseur G., Solomon S.: *Aeronomy of the Middle Atmosphere*. Springer, Dordrecht (2005)
9. Jackman C., DeLand M., Labow G., Fleming E., Weisenstein D., Ko M., Sinnhuber M., Russell J.: Neutral atmospheric influences of the solar proton events in October – November 2003. *Journal of Geophysical Research*, 110, A09S27 (2005)
10. T. Egorova, E. Rozanov, Y. Ozolin, A. Shapiro, M. Calisto, Th. Peter, W. Schmutz.: The atmospheric effects of October 2003 solar proton event simulated with the chemistry–climate model SOCOL using complete and parameterized ion chemistry. *Journal of Atmospheric and Solar-Terrestrial Physics*, 73 (2–3), 356–365 (2011)
11. https://sites.lebedev.ru/ru/DNS_FIAN/479.html, last accessed 2022/07/01
12. Bazilevskaya G., Kalinin M., Krainev M., Makhmutov V., Stozhkov Y., Svirzhetskaya A., Svirzhetsky N., Gvozdevsky B.: Temporal characteristics of energetic magnetospheric electron precipitation as observed during long-term balloon observations. *Journal of Geophysical Research: Space Physics*, 125, e2020JA028033 (2020)
13. Ozolin, Y.E., Karol’, I.L., Rozanov, E.V., Egorova T.A.: A model of the impact of solar proton events on the ionic and gaseous composition of the mesosphere. *Izvestiya, Atmospheric and Oceanic Physics*, 45, 737–750 (2009)
14. Porter H., Jackman C., Green A.: Efficiencies for production of atomic nitrogen and oxygen by relativistic proton impact in air. *The Journal of Chemical Physics*, 65, 154–167 (1976)
15. Sinnhuber M., Nieder H., Wieters N.: Energetic particle precipitation and the chemistry of the mesosphere/lower thermosphere. *Surveys in Geophysics*, 33 (6), 1281–1334 (2012)
16. Solomon S., Rusch D., Gérard J., Reid G., Crutzen P.: The effect of particle precipitation events on the neutral and ion chemistry of the middle atmosphere: II. Odd hydrogen. *Planet. Space Sci.*, 8, 885–893 (1981)

17. Verronen P., Andersson M., Marsh D., Kovács T., Plane J.: WACCM-D—Whole Atmosphere Community Climate Model with D-region ion chemistry. *Journal of Advances in Modeling Earth Systems*, 8, 954–975 (2016)
18. <https://www.spaceweatherlive.com/en/archive.html>, last accessed 2022/07/01